THEORY OF THE ELECTROKINETIC BEHAVIOR OF HUMAN ERYTHROCYTES

S. LEVINE, M. LEVINE, K. A. SHARP, AND D. E. BROOKS
Departments of Pathology, Chemical Engineering, and Chemistry, University of British Columbia, Vancouver, British Columbia, Canada V6T 1W5

ABSTRACT We develop a theory of electrophoresis of human erythrocytes that predicts mobilities significantly smaller than those based on the classical Smoluchowski relation. In the classical treatment the charge is assumed to be spread uniformly on the hydrodynamic surface. The present model takes into account that most of the charge, due mainly to sialic acid, is contained in the glycocalyx. The glycocalyx is modeled as a permeable layer of polyelectrolyte molecules anchored to the cell membrane. The charge is assumed to be uniformly distributed throughout this layer. The fluid flow in the layer is treated as being dominated by Stokes friction arising from idealized polymer segments. The Navier-Stokes equations are solved to give the dependence of electroosomotic velocity with distance from the cell surface. An expression for the electrophoretic mobility is obtained which contains two parameters (*a*) the thickness of the glycocalyx and (*b*) the mean polymer segment radius. The best fit to experimental data is obtained if these are given the values 75 Å and 7 Å, respectively. Deviation from experimental data at low ionic strength (<0.05 M) occurs. However, this deviation is in the direction one would expect if at low ionic strength the polyelectrolyte layer expands slightly due to decreased charge shielding.

INTRODUCTION

The well-known Smoluchowski formula for the velocity, U, of a charged, solid colloidal particle moving under an applied uniform electric field, E, through an aqueous electrolyte is

$$U = \epsilon E\zeta/4\pi\eta, \tag{1}$$

where ϵ and η are the dielectric constant and viscosity, respectively, of the electrolyte and ζ is the electrokinetic potential, defined as the potential at the nonslip or shear surface. Eq. 1 is valid for any insulating particle having a uniform potential and any size or shape provided the radius of curvature of its surface is large compared with the so-called thickness of the electric double layer. If the potential is sufficiently small to obey the linearized Poisson-Boltzmann or Debye-Huckel equation ($\lesssim$25 mV at 25°C), then we may write

$$\zeta = 4\pi\sigma/\epsilon\kappa, \tag{2}$$

where σ is the surface charge density, which is assumed to be uniform, and κ^{-1} is the Debye-Huckel thickness of the electric double layer. We obtain from Eqs. 1 and 2

$$\mu = U/E = \sigma/\eta\kappa, \tag{3}$$

where μ is the electrophoretic mobility of the colloidal particle.

The above relations have been widely applied to the electrophoresis of biological cells, in particular erythrocytes, even though the surfaces of these cells are very different from the interfaces of classical colloidal particles. There is good evidence from biochemical (Tomita and Marchesi, 1975) and electrokinetic (Heard and Seaman, 1960) studies that the dissociable chemical groups that make up the cell surface charge are distributed through a significant depth normal to the plane of the cell membrane. On human erythrocytes, the charges are borne by an extracellular layer of a variety of glycoproteins protruding from the membrane bilayer boundary known as the glycocalyx. The conformation of this mass at the cell surface is not known and therefore its thickness cannot be estimated precisely. However, it is likely that this conformation will depend on the ionic strength of the aqueous medium containing the cell and that the charge is not distributed uniformly. The carboxyl group of sialic acid is the main contributor to the net negative surface charge in this extracellular material. Because the pK of the carboxyl group is ~2.6, all the groups are ionized at physiological pH. All the erythrocyte sialic acid is present on the membrane surface and 95–100% of it can be removed by neuraminidase (Eylar et al., 1962). The action of this enzyme can be followed by assaying for free sialic acid in

Dr. S. Levine was previously affiliated with the Department of Mathematics, University of Manchester, Manchester, England.

Dr. M. Levine was previously affiliated with the Department of Biochemistry, University of Manchester, Manchester, England M13 9PL.

Address all correspondence to Dr. Brooks in the Department of Pathology.

the suspending medium and this provides a measurement of the total loss of charge from cell surfaces. The accompanying decrease in electrophoretic mobility of the cells can be measured independently and thus the theoretical expression (Eq. 3) can be tested. It is found that the amount of charge lost, as calculated from the change in mobility, is underestimated by a factor of 2 or 3 when compared with the amount of sialic acid released. In this paper, we propose to develop an alternative relation to Eq. 3 that will resolve the apparent contradiction.

We introduce a simple model of the extracellular mass coating the membrane bilayer of the erythrocyte (Fig. 1). We imagine that this layer of glycoprotein, glycolipid, and protein behaves as a plane layer of polyelectrolyte anchored to the membrane. In addition to the assumptions made in deriving the classical Smoluchowski expression, our model makes the following simplifying assumptions: (*a*) the net negative charge on the polyelectrolyte segments is replaced by an equivalent uniform charge distribution over a thickness, β. This thickness will be estimated by comparing plots of theoretical and experimental mobilities against ionic strength. This assumption ignores the discrete nature of the charge both parallel and perpendicular to the cell membrane. However it represents a significantly more realistic picture than the plane of uniform charge in the classical model, and allows a complete analytical treatment. (*b*) The solvent (water) and small mobile ions are able to penetrate between the segments of the polyelectrolyte layer; κ, the shielding constant, η, the fluid viscosity, and ϵ, the dielectric constant are assumed to have the same values as in the bulk suspending medium. That is, no ion exclusion of the types considered by Haydon (1961) or Brooks (1973) are considered. (*c*) Under the action of an applied electric field, E, these ions move between the segments, carrying solvent molecules with them. This fluid flow is isotropic.

The Navier-Stokes equations for the hydrodynamic flow through the polyelectrolyte layer have a force term that describes the resistance exerted by the polyelectrolyte segments on this flow. This term is taken from theories of

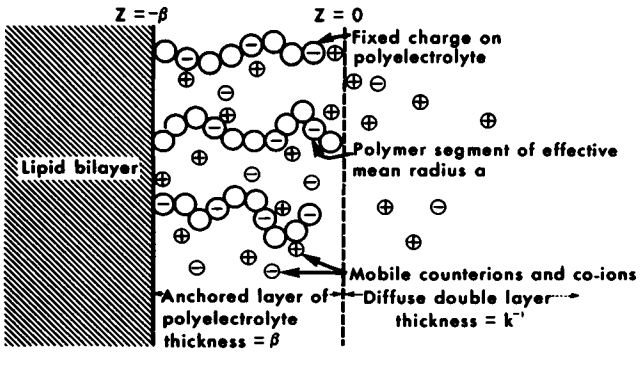

FIGURE 1 Model of the erythrocyte surface analyzed in the present work. The fixed charge density borne by the polyelectrolyte is assumed uniform through the volume of the layer.

the frictional properties of dilute, uncharged polymer solutions due to Brinkman (1947), Kirkwood and Riseman (1948), Debye and Beuche (1948), and more recently Felderhof and Deutch (1975) and Deutch and Felderhof (1975). This model has been applied to the electrophoresis of charged colloidal particles coated with uncharged polymers or polyelectrolytes by Levine and Jones (1978), and with charged polymers or polyelectrolytes by Jones (1979). Although the segments in the extracellular layer are heterogeneous, for simplicity the segments in the polyelectrolyte layer model will be treated as equal spheres with a friction coefficient based on the Stokes expression for a single solid sphere moving through a Newtonian liquid. Strictly, the Stokes formula is a valid assumption only when the separation between the segments is much larger than the segment radius. We have therefore chosen a Stokes effective mean radius that must be regarded as empirical. It will be assumed initially that this Stokes radius is identical with the radius of a segment based on density considerations, which is discussed in the section entitled Numerical Assignment to Parameters in the Mobility Analysis of Human Erythrocyte. The actual radius chosen can be adjusted to fit the experimental cell mobility curve as a function of the ionic strength.

Derivation of the Electrophoretic Mobility of the Erythrocyte

As explained in the Introduction, we choose a plane layer of polyelectrolyte, anchored to the membrane, as a model for the glycocalyx protruding from the membrane bilayer boundary. The net negative charge on the segments of the polyelectrolyte is replaced by an equivalent uniform charge distribution of volume density, ρ_e. Hence, if β is the thickness of the charged part of the polyelectrolyte, the resulting surface charge density is $\sigma = \rho_e\beta$. This charge is partly screened by the small, mobile ions of electrolyte in the suspending medium, which are able to penetrate the polyelectrolyte layer. Choosing coordinates fixed to the membrane, a uniform electric field, E, is applied in the x-direction parallel to the plane of the membrane boundary. The solvent molecules and small ions of the supporting electrolyte flow between the segments of the polyelectrolyte parallel to the x-axis under the influence of this field. These segments have a uniform mean volume density, N, and their frictional force on the fluid flow is described by a common effective Stokes radius, a. We choose the z-axis as normal to the plane of the membrane such that $z = 0$ is the boundary between the polyelectrolyte layer and the diffuse layer of small ions situated between the polyelectrolyte layer and the bulk of the supporting electrolyte. The plane $z = -\beta$ is assumed to mark both the inner boundary of the uniform charge distribution and the nonslip or shear plane of the hydrodynamic flow (Fig. 1). We need not specify the precise position of the shear plane, relative to the membrane bilayer boundary, although we expect that the distance from this barrier is of molecular dimensions.

For small values of the mean electrostatic potential $\psi = \psi(z)$ ($\leq$25 mV at T = 25°C) relative to the bulk electrolyte (at $z = \infty$), the linearized Poisson-Boltzmann equations for the polyelectrolyte and diffuse layers are, respectively,

$$\frac{\partial^2\psi}{\partial z^2} - \kappa^2\psi(z) = \frac{-4\pi\rho_e}{\epsilon}, \quad -\beta < z < 0 \tag{4}$$

$$\frac{\partial^2\psi(z)}{\partial z^2} - \kappa^2\psi(z) = 0, \quad z > 0 \tag{5}$$

subject to the boundary conditions

$$\psi(z), \frac{\partial\psi}{\partial z} \text{ continuous} \tag{6}$$

at $z = 0$,

$$\frac{\partial\psi}{\partial z} = 0 \tag{7}$$

at $z = -\beta$, and

$$\psi \longrightarrow 0 \tag{8}$$

as $z \longrightarrow \infty$. The solutions are

$$\psi(z) = \alpha + Ae^{-\kappa z} + Be^{\kappa z}, \quad -\beta \leq z \leq 0$$
$$\psi(z) = Ce^{-\kappa z}, \quad z \geq 0, \tag{10}$$

where

$$\alpha = \frac{4\pi\rho_e}{\epsilon\kappa^2} = \frac{4\pi\sigma}{\epsilon\kappa(\kappa\beta)} \tag{11}$$

and

$$A = -\frac{\alpha}{2}e^{-2\kappa\beta}, \quad B = \frac{-\alpha}{2}, \quad C = A - B. \tag{12}$$

The potential at the shear plane $z = -\beta$ is

$$\psi(-\beta) = \alpha(1 - e^{-\kappa\beta}) \tag{13}$$

and at the edge of the polyelectrolyte layer, $z = 0$

$$\psi(0) = \frac{\alpha}{2}(1 - e^{-2\kappa\beta}). \tag{14}$$

For $\kappa\beta \gg 1$, $\psi(0)$ is nearly $\frac{1}{2}\psi(-\beta)$. For $\kappa\beta \gg 1$, Eq. 13 yields a potential at the nonslip plane that, for a given σ, is smaller than the classical formula (Eq. 2) by a factor exceeding $\kappa\beta$. This property has the effect of extending the range of validity of the linearized Poisson-Boltzmann equation.

Let us now consider the steady-state electroosmotic fluid flow due to the applied electric field, E, in the x-direction. The Navier-Stokes equations are

$$\eta\frac{\partial^2 u(z)}{\partial z^2} + \rho(z)E = 0, \quad z > 0 \tag{15}$$

$$\eta\frac{\partial^2 u}{\partial z^2} + \rho(z)E - Nfu(z) = 0, \quad -\beta < z < 0 \tag{16}$$

where

$$\rho(z) = \frac{-\epsilon}{4\pi}\frac{\partial^2\psi(z)}{\partial z^2} \tag{17}$$

and

$$f = 6\pi\eta a \tag{18}$$

is the effective Stokes friction. References to this term have been quoted in the Introduction.

The following boundary conditions hold:

$$u = 0 \tag{19}$$

at $z = -\beta$

$$u, \frac{\partial u}{\partial z} \text{ continuous} \tag{20}$$

at $z = 0$.

Eqs. 15 and 16 can be integrated, and the appropriate expressions for the potentials, Eqs. 9 and 10, substituted in. Applying the boundary conditions, Eqs. 19 and 20, and equating the value of u as $z \longrightarrow \infty$ as equal and opposite in sign to the electrophoretic velocity, we obtain for the cell mobility, μ

$$\mu = \frac{\sigma}{2\eta\kappa(\kappa\beta)}\left\{-(1 - e^{-2\kappa\beta})\left(1 + \frac{\kappa}{\gamma}\tanh\gamma\beta\right) - 2\frac{\kappa^2}{\gamma^2}\left(1 - \frac{1}{\cosh\gamma\beta}\right) + \frac{\kappa^2}{(\kappa^2 - \gamma^2)}\left[-1 - e^{-2\kappa\beta} + \frac{\kappa}{\gamma}(1 - e^{-2\kappa\beta})\tanh\gamma\beta + \frac{2e^{-\kappa\beta}}{\cosh\gamma\beta}\right]\right\} \tag{21}$$

where $\gamma^2 = Nf/\eta = 6\pi aN$ and N is the mean number of polymer segments per unit volume. Since we find that $\kappa\beta$, $\gamma\beta$ lie in the range 2–10, Eq. 21 predicts smaller mobilities than those predicted by Eq. 3.

We now compare Eq. 21 with the resulting mobilities from two other limiting charge distributions. (*a*) All the charge is located at $z = 0$, the boundary of the diffuse layer and the polyelectrolyte. This model differs only in the form of the potential distribution $\psi(z)$, Eqs. 9 and 10, and the boundary condition (Eq. 6). For this model, we state without proof

$$\mu = \frac{\sigma}{2\eta\kappa}\left[-(1 + e^{-2\kappa\beta})\left(1 + \frac{\kappa}{\gamma}\tanh\gamma\beta\right) + \frac{\kappa^2}{(\kappa^2 - \gamma^2)} \cdot \left(-1 + e^{-2\kappa\beta} - \frac{\kappa}{\gamma}(1 - e^{-2\kappa\beta})\tanh\gamma\beta - \frac{2e^{-\kappa\beta}}{\cosh\gamma\beta}\right)\right] \tag{22}$$

(*b*) Similarly, if all the charge is located at $z = -\beta$, i.e., at the membrane bilayer, the boundary condition (Eq. 7) is altered, giving

$$\mu = \frac{\sigma}{\eta\kappa(\kappa^2 - \gamma^2)}\left[\gamma^2\left(1 + \frac{\kappa}{\gamma}\tanh\gamma\beta\right)e^{-\kappa\beta} - \frac{\kappa^2}{\cosh\gamma\beta}\right], \tag{23}$$

which is identical to the result obtained by Levine and Jones (1978).

Numerical Assignment to Parameters in the Mobility Analysis of the Human Erythrocyte

In addition to the viscosity, η, the dielectric constant, ϵ, and the Debye-Huckel parameter, κ, which we assume equal to their values in the suspending medium, we require values of four other parameters. These are σ, the surface charge density, β the thickness of the polyelectrolyte layer, N the average number of polyelectrolyte segments per unit volume, and a, the Stokes effective mean radius of the segment. In estimating these quantities, we used several publications on the surface properties of human erythrocyte and crosschecked for consistency. The wide range of relevant published data is, to some extent, a reflection of the different methods of analysis and the difficulties involved in the measurements.

Charge, σ, per Unit Area of the Cell

As mentioned in the Introduction, the carboxyl group of sialic acid is mainly responsible for the negative surface charge and is fully ionized at physiological pH. The number of molecules of sialic acid per area varies linearly with the mobility among erythrocytes from different species studied (Eylar et al., 1962). Analyses of sialic acid estimated at the surface have been tabulated by Cook (1976). Although there is a wide variation, the mean corresponds well with the average value of 17.7 ± 1.5 fg/cell for the sialic acid (mol wt 309.3) released by *Vibrio cholerae* neuraminidase from whole human red cell populations as reported by Seaman et al. (1977). The estimate therefore is $17.7 \times 10^{-15} \times 6.02 \times 10^{23}/309.3 = 3.45 \times 10^{7}$ molecules/erythrocyte. The surface area was taken as 155 μm^2 (Whittam, 1964), which is close to the mean of two values tabulated by Weinstein (1974), namely 163 μm^2 (Ponder, 1948) and 145 μm^2 (Westerman et al., 1961). The number of sialic acid molecules/cm^2 = 2.22×10^{13} and $\sigma = 2.22 \times 10^{13} \times 4.80 \times 10^{-10} = 1.065 \times 10^{4}$ esu cm^{-2}.

Thickness, β, of the Extracellular Surface Layer

A good estimate of β is not available. Furthermore, expansion of the polypeptide chains can be assumed at low ionic strength. Jenkins and Tanner (1977) report that the structure of Band 3 depends on the ionic strength of the medium, with a tighter structure at physiological ionic strengths than under low ionic strength conditions. Examination of ghost cell surface ultrastructure has demonstrated the presence of plaques $\sim 0.3 \times 10^{-6}$ cm thick (Hillier and Hoffman, 1953). However it has been suggested by Weinstein (1974) that the Hoffman plaques could be due to collapse of glycoprotein molecules resulting from the surface tension forces of evaporating water introduced during air-drying. Up to the present, all attempts to measure β have been subject to artifacts. We have calculated mobilities assigning β equal to 0.50×10^{-6} cm, 0.75×10^{-6} cm, and 1.0×10^{-6} cm to observe the effect of variations in this parameter.

Division of the Surface Mass into Segments and Determination of Parameter N

We have already explained the use of the mean segment radius, a, when describing the frictional properties of the polyelectrolyte layer to fluid flow. Given the radius of a segment, the number of segments cm^{-3}, N, may be calculated if the mass of (*a*) carbohydrate and (*b*) protein at the surface of the erythrocyte is known.

Carbohydrate mass. The carbohydrate composition of the human erythrocyte membrane is given as 165 μg carbohydrate/mg protein (Robinson, 1975). Since the total protein is 52% of membrane mass (Steck, 1974) and the hemoglobin-free ghost mass is ~ 11–12×10^{-13} g (Dodge et al., 1963), then the carbohydrate mass is ~ 0.94–1.02×10^{-13} g or 8.5% carbohydrate (of the total membrane mass). Other references report carbohydrate as 7.2% of total ghosts (Pennell, 1974), 8–10% (Tanner, 1978), and 8% (Steck, 1974). Taking the estimate of carbohydrate as 8.5% of the total membrane mass gives a value of 0.98×10^{-13} g for total carbohydrate, all of which is assumed to be extracellular. The major portion of the carbohydrate attached to the erythrocyte membrane seems to be organized into high molecular weight glycan structures. Some of these glycans are attached to lipids; the glycolipid fraction (the globosides and hematosides) accounts for 5–10% by weight of the total lipids, i.e., $0.25 - 0.50 \times 10^{-13}$ g. There are several million molecules of glycolipid per cell (Sweeley and Dawson, 1969). However the majority of the glycans are attached to protein (Jarnefelt et al., 1978), which we now consider.

Protein mass at the extracellular surface. Not all the surface proteins have yet been characterized. The best known is glycophorin A, an integral membrane protein that projects from the bilayer surface. Somewhat less well known is another integral membrane protein, Band 3. However the major contribution to the mass on the surface of the cell is carbohydrate. There are four identified glycoproteins in the erythrocyte membrane: (*a*) glycophorins A, B, C, (*b*) Band 3; (*c*) PAS 2′, (*d*) PAS 3, and other minor glycoproteins. The glycophorins A, B, and C and Band 3 are the major glycoproteins, while PAS 2′ and PAS 3 are minor (Tanner, 1978).

Glycophorin A. The complete primary structure of this molecule has been described by Tomita and Marchesi (1975). The monomer has a molecular weight of 31,000 and is 60% carbohydrate. About 80% of the total

mass of glycophorin A is at the surface and 75% of the glycosylated surface segment is carbohydrate. Taking the number of molecules of glycophorin A monomer as 400,000/cell (Furthmayr, 1978), then the mass of glycophorin A per cell is equal to 0.206×10^{-13} g, the mass on the surface is 0.165×10^{-13} g, and the mass of the protein portion at the surface is 0.0412×10^{-13} g. Carbohydrate contributed by glycophorin A is 0.124×10^{-13} g, accounting for only 12.6% of the total carbohydrate or ~20% of the glycoprotein carbohydrate. A substantial fraction of the carbohydrate is contributed by the glycolipids, ~21–42%. Glycophorin A accounts for only 40% of the sialic acid. Glycophorin B and C, which have recently been isolated (Furthmayr, 1978), are also sialoglycoproteins, the number of polypeptide copies per cell estimated as 70,000 and 35,000, respectively, compared with 400,000 copies of glycophorin A. Glycophorin B appears to be structurally similar to glycophorin A. Clearly, other sialoproteins are, at present, unidentified.

Band 3. Band 3 is estimated to have a molecular weight of 90,000. There are 10^6 peptides per cell (1.5×10^{-13} g) of which 7% is carbohydrate, but the proportion of protein at the extracellular surface is not known. Because so little is known of the amounts of remaining surface proteins, we have used an approximate estimate of 0.2×10^{-13} g for the total extracellular surface protein and taken the total mass on the surface of the cell as $\sim 1.18 \times 10^{-13}$ g. The mean number of segments cm^{-3} is equal to

$$N = \frac{\text{total mass on the surface}}{\text{mass of a segment}} \times \frac{1}{V},$$

where V is the volume of the layer, i.e., the area of the cell multiplied by β, the thickness of the surface mass. The mass of a segment equals $\frac{4}{3}\pi a^3 \bar{v}^{-1}$. The value of $\bar{v}$, the partial specific volume, was taken as 0.611 $cm^3 g^{-1}$, which is the partial specific volume of dextran (Granath, 1958), i.e., the effective polymer segment density is equal to 1.637 g cm^{-3}. Introducing the total mass and surface area of the cell, N is therefore related to a and β by the relation

$$N = 1.11 \times 10^{-8}/\beta a^3. \qquad (24)$$

The parameter, γ, therefore also depends on a and β. We shall vary a and β to obtain a fit between the theoretical and experimental mobility curves.

NUMERICAL RESULTS AND DISCUSSION

Figs. 2–4 show plots of Eq. 21 for the mobility, μ, (in $\mu m\ s^{-1}\ V^{-1}$ cm) against ionic strength, c (c is concentration in mol l^{-1} with a 1-1 electrolyte, for which $\kappa = [10^8 c^{1/2}/3.04]$ cm^{-1} at $T = 25°C$). Three different values of the layer thickness, β, and a range of the segment radii, a, from 4×10^{-8} to 8×10^{-8} cm have been chosen. Comparison with the experimental results (solid curve) shows that of the three values, $\beta = 0.75 \times 10^{-6}$ cm gives the best overall fit

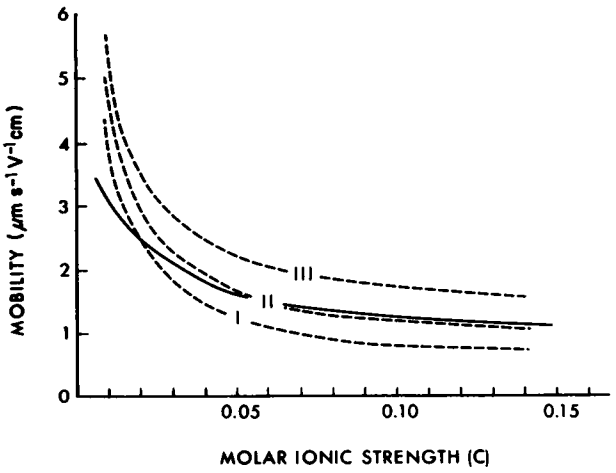

FIGURE 2 Plot of mobility of erythrocyte in $\mu m\ s^{-1}V^{-1}$ cm vs molar ionic strength, c, where for a 1-1 electrolyte at $T = 25°C$, the Debye-Huckel parameter $\kappa = (10^8 c^{1/2}/3.04)cm^{-1}$. Broken curves were calculated using Eq. 21 for layer thickness $\beta = 0.05 \times 10^{-6}$ cm and segment radii $a = 4$, 6, and 8×10^{-8} cm (curves I, II, and III, respectively). Surface charge density $\sigma = 1.065 \times 10^4$ esu $cm^{-2} = 3.55\ \mu C\ cm^{-2}$ and N is given by Eq. 24. The variation of dielectric constant and viscosity with electrolyte concentration at $T = 25°C$ is taken into account through the formulae $\epsilon = 78.36 - 11.0\ c$, $\eta = (0.89 + 0.084\ c) \times 10^{-2}$. The solid curve shows the experimental results.

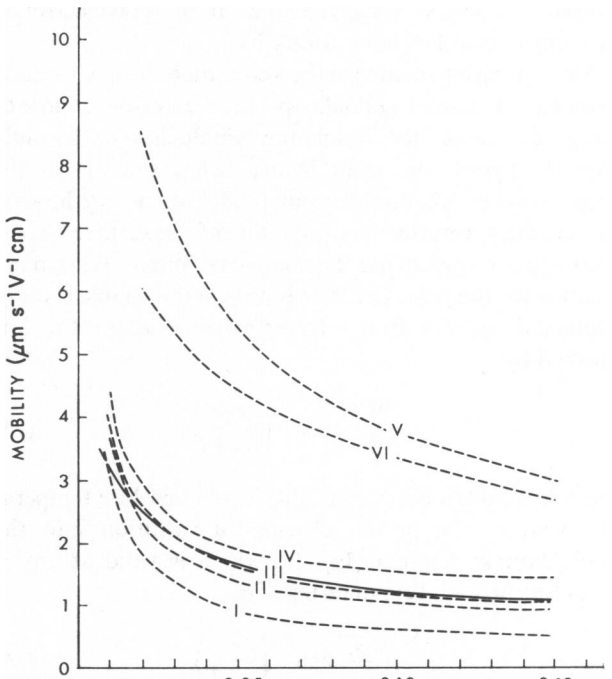

FIGURE 3 Mobility-ionic strength plots similar to those in Fig. 1 for $\beta = 0.75 \times 10^{-6}$ cm and $a = 4$, 6, 7, and 8×10^{-8} cm (broken curves I–IV). Curves V and VI are the corresponding plots of Eqs. 3 and 26, respectively, choosing the same σ as for the erythrocyte; these are applicable to a charged colloidal particle. The solid curve is the experimental.

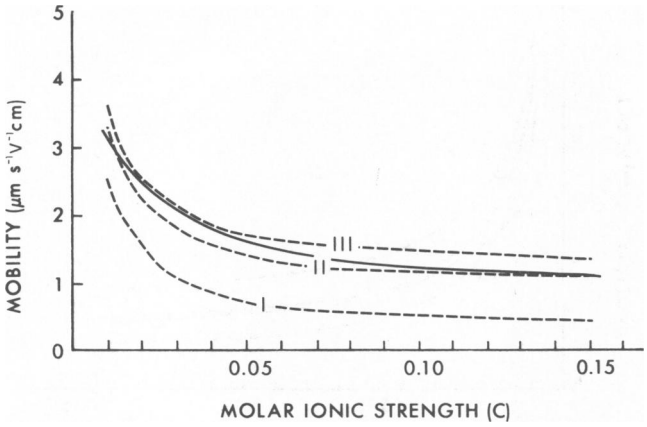

FIGURE 4 Mobility-ionic strength plots similar to those in Fig. 1 for $\beta = 1.00 \times 10^{-6}$ cm and $a = 4$, 7, and 8×10^{-8} cm (broken curves I–III). The solid curve is the experimental.

at $\sim a = 7 \times 10^{-8}$ cm. Good agreement with experimental results can also be obtained at the higher ionic strengths for $\beta = 0.5 \times 10^{-6}$ cm and $a = 6 \times 10^{-8}$ cm, but a deviation develops below $c = 0.05$. The third thickness, $\beta = 10^{-6}$ cm, is least satisfactory in reproducing the general shape of the experimental curve over the whole range of c for any a. However, a comparison of the results with the three values of β strongly suggests that even better agreement with experimental result is obtained at low $c(\lesssim 0.02$ M) if β is allowed to increase somewhat, i.e., if the polyelectrolyte layer expands at low ionic strengths.

We now wish to compare the above mobilities with those obtained for a solid colloidal particle carrying a surface charge density σ, for which the Smoluchowski formula (Eq. 1) applies. We shall justify below the use of the Debye-Huckel potential for our model of the erythrocyte surface. However, for the same value of the surface charge density, σ, we need to use the nonlinear Poisson-Boltzmann equation for the potential distribution in the double layer of a colloidal particle. In a 1-1 electrolyte medium, Eq. 2 is replaced by

$$\zeta = \frac{2kT}{e} \sinh^{-1}\left(\frac{2\pi e\sigma}{\epsilon\kappa kT}\right), \tag{25}$$

where k is Boltzmann's constant, T, the absolute temperature, and e, the proton charge. Substitution into the Smoluchowski relation (Eq. 1), which is valid at any ζ, yields for the mobility, in terms of σ,

$$\mu = \frac{\epsilon kT}{2\pi\eta e} \sinh^{-1}\left(\frac{2\pi e\sigma}{\epsilon\kappa kT}\right). \tag{26}$$

In Fig. 3 we have also plotted as functions of ionic strength both the linear form (Eq. 3) and the more exact relation (Eq. 26) for the mobility of the colloidal particle, using the values of σ and κ from the erythrocyte data. It is seen that the mobilities based on the Smoluchowski formula (Eq. 1) exceed by a factor of 2 or 3 the experimental results for erythrocytes.

A study of the potential distribution provides further information on the differences between our model of the erythrocyte surface and the double layer of the classical colloidal particle. In Fig. 5, we have plotted as functions of ionic strength, the potential $\psi(-\beta)$ at the nonslip plane (Eq. 13), and the potential $\psi(0)$ at the limit of the diffuse layer (Eq. 14). These are compared for the same σ and variation in κ with the double layer potentials for classical colloids, as given by Eq. 2, using the Debye-Huckel equation, and by Eq. 26, using the Poisson-Boltzmann equation. It is striking that the surface potentials $\psi(-\beta)$ and $\psi(0)$ are well below those predicted by the classical Eqs. 2 or 26 and indeed, except at low ionic strengths, lie within the Debye-Huckel limits. There is no contradiction between the value of σ due to the ionized sialic acid and the small values of the potentials $\psi(-\beta)$ and $\psi(0)$, because the charge, σ, is partly neutralized by the net charge due to the small ions that are contained in the polyelectrolyte layer. To demonstrate this property, consider the net charge per unit cross-sectional area of the diffuse layer, namely

$$\sigma_d = \frac{\epsilon}{4\pi}\left(\frac{d\psi}{dz}\right)_{z=0} = \frac{-\sigma}{2\beta\kappa}(1 - e^{-2\kappa\beta}), \tag{27}$$

where $\psi(z)$ is given by Eq. 10. Noting that $\kappa\beta$ lies between 2 and 10, $|\sigma_d| \ll \sigma$ and therefore by electrical neutrality,

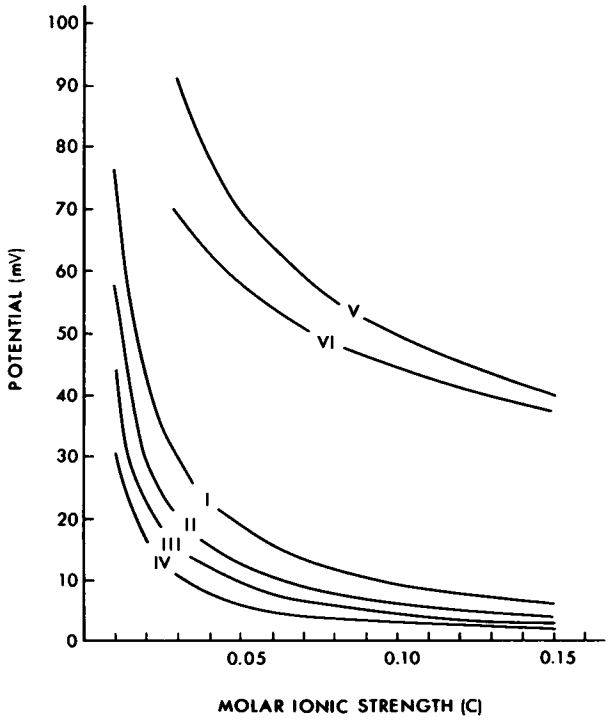

FIGURE 5 Plots of potentials at nonslip plane ($z = -\beta$) and at outer boundary of polyelectrolyte layer ($z = 0$) as functions of ionic strength. Curves I, II: $\psi(-\beta)$ at nonslip plane; $z = -\beta$ for $\beta = 0.5$ and 0.75×10^{-8} cm, respectively. Curves III, IV: $\psi(0)$ at the outer boundary; $z = 0$ for $\beta = 0.5$ and 0.75×10^{-8} cm, respectively. Curves V, VI: zeta potential given by Eqs. 2 and 25, respectively, for a colloidal particle, choosing erythrocyte σ.

most of the sialic acid charge is compensated by the small mobile ions in the polyelectrolyte layer.

In Fig. 6 we have plotted mobility-ionic strength curves for the three different charge distributions in the polyelectrolyte layer, which are based on Eqs. 21–23 (curves I, II, and III, respectively) for $\beta = 0.75 \times 10^{-6}$ cm and $a = 7 \times 10^{-8}$ cm. When compared with our model of a uniform sialic acid charge distribution in the polyelectrolyte layer (curve I), at the higher ionic strengths the mobility is seen to be high when the charge is concentrated at the limit of the diffuse layer, $z = 0$ (curve II), and low when situated at the shear plane, $z = -\beta$ (curve III). Indeed curve II in Fig. 6 shows a higher mobility than curves V or VI in Fig. 3, which describe the corresponding Smoluchowski mobility for the same charge density located on a solid colloidal surface in the absence of a polyelectrolyte layer. In Fig. 7, the ratio $u(z)/E$ is shown as a function of z for our uniform net charge model of the polyelectrolyte layer, at ionic strengths $c = 0.05$ to 0.15 M. These curves are calculated from Eqs. 15 and 16. We see that the velocity profile within the polyelectrolyte layer is virtually independent of the ionic strength. It is almost completely controlled by the resistance of the polymer segments in spite of significant differences in this region in potential, and hence body force, as a function of ionic strength.

Because of the frictional force exerted by the polyelectrolyte segments on solvent motion, one might first expect that for a given σ, the Smoluchowski mobility in the absence of the polyelectrolyte layer should exceed the mobility calculated for the case in which σ is concentrated at the outer limit of the polymer layer at $z = 0$. The opposite is true, however, at the higher ionic strengths. This occurs because, in our model, since ions and fluid penetrate in and behind the charge plane, the fluid velocity is not constrained to be zero at this location. Thus for a given body force there is more electroosmosis, resulting in $U(z)$, $z \rightarrow \infty$ being larger, and hence the mobility being larger.

It is also of interest to consider the potential at the nonslip plane, the zeta potential, for the various models. For the Smoluchowski model this is given by Eq. 2. A comparison of this expression with the mobility expression (Eq. 21) shows that there is no simple relationship between mobility and zeta potential. Thus in our model the zeta potential has no special significance in determining the mobility, whereas the physical characteristics of the surface are crucial.

The present model of cell electrophoresis, which leads to Eq. 21, provides a value for the human erythrocyte surface potential that is much lower than that calculated from the Smoluchowski relationship (Eq. 1). Examination of Eq. 9 shows that at $z = 0$ the potential is only ~3 mV, whereas the value commonly accepted, derived from Eq. 1, is ~16 mV at this salt concentration. It therefore seems highly likely that the electrostatic surface potential, which is believed to be important in stabilizing red cells in suspension via electrostatic repulsion, is in fact rather small and is unlikely to be responsible for the fact that these cells do not aggregate in the absence of added macromolecules.

In addition to their fidelity with the measured mobility-ionic strength curve, further evidence supporting the predictions of our model comes from Uzgiris and Fromageot (1976), who measured the hydrodynamic thickness of protein films adsorbed on polystyrene latex spheres. The

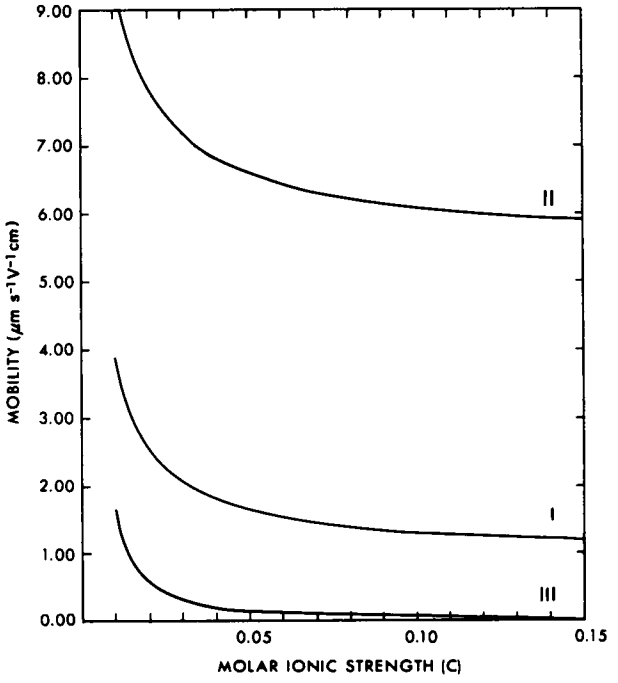

FIGURE 6 Mobility-ionic strength plots for three different charge distributions in polyelectrolyte layer, for $\beta = 0.75 \times 10^{-6}$ cm and $a = 7 \times 10^{-8}$ cm. Curve I is based on Eq. 21, i.e., for uniform sialic acid charge density in the layer; curve II on Eq. 22, i.e., for equivalent surface charge density, σ, on outer boundary $z = 0$; curve III on Eq. 23, i.e., for equivalent surface change density at inner boundary, $z = -\beta$.

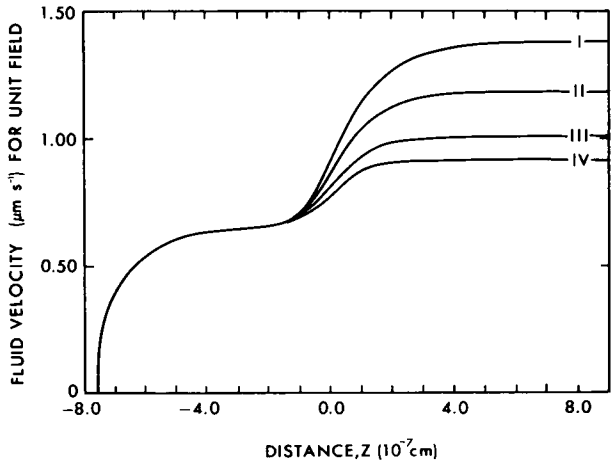

FIGURE 7 Plot of ratio $u(z)/E$ (fluid velocity per electric field) in $\mu m\ s^{-1}\ V^{-1}$ cm, as a function of z, where $u(z)$ is given by Eqs. 15 and 16, i.e., for the model of uniform sialic acid charge distribution in polyelectrolyte layer. Curves I, II, III, and IV refer to ionic strengths of 0.05, 0.07, 0.11, and 0.15 M, respectively; $\beta = 0.75 \times 10^{-6}$ cm and $a = 7 \times 10^{-8}$ cm.

proteins used were (*a*) glycoprotein isolated from human red blood cells by procedures that yielded the major sialoglycoprotein and (*b*) serum albumins, both human and bovine. The thickness of adsorbed glycoprotein was found to be 120 ± 15 Å compared with ~30 Å for the thickness of adsorbed serum albumins. The authors suggest an end-on orientation for the human red blood cell glycoprotein, which is of course consistent with our model. The latex spheres appear to have been suspended in 5 mM NaCl, in the region where the deviation from our theory occurs. We have suggested in the section on Numerical Assignment to Parameters that the polyelectrolyte layer expands at such low ionic strength. In addition the major sialoglycoprotein of the red cell has a transmembrane orientation with 80% of its total mass at the surface. Thus the thickness adsorbed at the surface of the latex spheres would be expected to be somewhat greater than that at the red cell surface. The authors suggest that the molecules are affixed via their hydrophobic ends onto the hydrophobic parts of the polystyrene surface.

It is also of interest to compare the surface coverage, packing density, and volume fraction obtained for the glycoprotein film on latex spheres with that calculated from our data on the red cell surface (Table I). The coincidence is striking, suggesting that the thickness and fractional volume filling deduced from our model are reasonable.

An independent measure of $\psi(0)$ would be useful, but we are not aware of any technique that would provide such data. Qualitative support for the idea that all of the cell surface sialic acid contributes to some extent to the mobility exists, however. If mobility measurements are made at various times during a neuraminidase digestion of human erythrocytes, and the amount of sialic acid hydrolyzed is measured in parallel, it is found that at all stages of digestion the fractional mobility change is directly proportional to the amount of sialic acid released (Luner et al., 1975). These results are consistent with the results of our analysis and support the basic premise that fluid flow must occur within the glycocalyx of the cell during electrophoresis.

TABLE I
GLYCOPROTEIN FILM ON LATEX SPHERE COMPARED WITH RED CELL SURFACE

	Glycoprotein film on latex spheres*	Mass on red cell surface‡
Surface coverage ($mg\ m^{-2}$)	0.75	0.76
Packing density ($g\ cm^{-3}$) 0.10 (75 Å thickness)	0.06	0.076 (100 Å thickness)
Volume fraction (density = 1.6)	4%	5% (100 Å thickness)
	—	6% (75 Å thickness)

*Uzgiris and Fromageot (1976).
‡From our calculations, total mass = 1.18×10^{-13}g.

It has been known for some time that neuraminidase-treated human erythrocytes show a residual negative electrophoretic mobility of ~30% (Vassar et al., 1973). The source of the additional negative groups has yet to be unequivocally identified. It could well be that removal of the sialic acid groups causes an alteration of the molecular configuration of the remaining glycoprotein resulting in exposure of negatively charged groups undetected in the intact molecule. Alternatively, a residual electrophoretic mobility is quite possible even if the net charge of the ionic groups remaining after the removal of the sialic acid groups is zero, a property often overlooked in the literature. An extreme but simple example is provided by the model where the two boundaries $z = 0$ and $z = -\beta$ carry surface charge densities σ and $-\sigma$, respectively, and uncharged polymer is situated between these boundary charges. Because our equations for the potential and fluid velocity are linear, we need only subtract Eq. 22 from Eq. 23 to obtain the electrophoretic mobility for such a model. This is illustrated graphically in Fig. 6, where we take the difference of curves II and III. The reason that a residual mobility at $\sigma = 0$ does not appear in our Eq. 21 is that we have assumed a uniform distribution of charged polyelectrolyte segments. In other words, a nonuniform distribution of charged segments normal to the cell membrane would yield in general a residual mobility when the net charge is zero. Other than the limiting planar layers of charge considered above, we shall not consider any other nonuniform distribution of charge, because the true distribution on the cell membrane is not known.

We are grateful for financial assistance from the Medical Research Council of Canada and the Faculty of Medicine of the University of British Columbia. Dr. M. Levine would like to thank the Departmental Board, Department of Biochemistry, University of Manchester, for granting leave of absence. Dr. M. Levine and Dr. S. Levine are grateful to the Department of Pathology, University of British Columbia for providing facilities.

Received for publication 29 December 1979 and in final form 30 November 1982.

Note Added in Proof: Since this work was completed two very similar treatments have been published by Donath and Pastushenko, 1979 (*Bioelectrochem. Bioenerg.* 6:543–554) and Wunderlich, 1982 (*J. Colloid Interface Sci.* 88:385–397).

REFERENCES

Brinkman, H. C. 1947. Calculation of the viscosity and the sedimentation constants for solutions of large chain molecules. *Physika.* 13:447–448.

Brooks, D. E. 1973. The effect of neutral polymers on the electrokinetic potential of cells and other charged particles. II. A model for the effect of adsorbed polymer on the diffuse double layer. *J. Colloid Interface Sci.* 43:687–699.

Cook, G. M. W. 1976. Analysis of membrane carbohydrates. *In* Biochemical Analysis of Membranes. A. H. Maddy, editor. John Wiley and Sons, Inc., New York. 311.

Debye, P., and A. Bueche. 1948. Intrinsic viscosity, diffusion and sedimentation rate of polymers in solution. *J. Chem. Phys.* 16:573–579.

Deutch, J. M., and B. U. Felderhof. 1975. Frictional properties of dilute polymer solutions. II. The effect of preaveraging. *J. Chem. Phys.* 62:2398–2405.

Dodge, J. T., C. Mitchell, and D. J. Hanahan. 1963. Preparation of hemoglobin-free ghosts of human erythrocytes. *Arch. Biochem. Biophys.* 100:119–130.

Eylar, E. H., M. A. Madoff, O. V. Brody, and J. L. Oncley. 1962. The contribution of sialic acid to the surface charge of the erythrocyte. *J. Biol. Chem.* 237:1992–2000.

Felderhof, B. U., and J. Deutch. 1975. Frictional properties of dilute polymer solutions. I. Rotational friction coefficient. *J. Chem. Phys.* 62:2391–2397.

Furthmayr, H. 1978. Glycophorins A, B and C: a family of sialoglycoproteins. Isolation and preliminary characterization of trypsin-derived peptides. *J. Supramol. Struct.* 9:79–95.

Granath, K. 1958. Solution properties of branched dextrans. *J. Colloid Sci* 13:308–328.

Haydon, D. A. 1961. The surface charge of cells and some other small particles as indicated by electrophoresis. I. The zeta potential-surface charge relationships. *Biochim. Biophys. Acta.* 50:450–457.

Heard, D. H., and G. V. F. Seaman. 1960. The influence of pH and ionic strength on the electrokinetic stability of the human erythrocyte membrane. *J. Gen. Physiol.* 43:635–654.

Hillier, J., and J. F. Hoffman. 1953. Ultrastructure of plasma membrane. *J. Cell Comp. Physiol.* 42:203–220.

Jarnefelt, J., J. Rush, Y. Li, and R. A. Laine. 1978. Erythroglycan, a high molecular weight glycopeptide with the repeating structure (galactosyl (1 → 4)-2-deoxy-2-acetamido-glucosyl (1 → 3)) comprising more than one-third of the protein-bound carbohydrate of human erythrocyte stroma. *J. Biol. Chem.* 253:8006–8009.

Jenkins, R. E., and M. J. A. Tanner. 1977. Ionic-strength dependent changes in the structure of the major protein of the human erythrocyte membrane. *Biochem. J.* 161:131–138.

Jones, I. S. 1979. A theory of electrophoresis of large colloid particles with adsorbed polyelectrolyte. *J. Colloid Interface Sci.* 68:451–461.

Kirkwood, J. G., and J. Riseman. 1948. The intrinsic viscosities and diffusion constants of flexible macromolecules in solution. *J. Chem. Phys.* 16:565–573.

Levine, S., and I. S. Jones. 1978. *Faraday Discuss. Chem. Soc.* 65:337.

Luner, S. J., P. Sturgeon, D. Szklarek, and D. T. McQuiston, 1975. Effects of proteases and neuraminidase on RBC surface charge and agglutination. *Vox Sang.* 28:184–199.

Pennell, R. B. 1974. Composition of normal human red cells. *In* Red Blood Cell. D. M. Surgenor, editor. Academic Press, Inc., New York and London. 1:93–146.

Ponder, E. 1948. Hemolysis and Related Phenomena. Grune and Stratton, Inc., New York. 14.

Robinson, G. B. 1975. The isolation and composition of membranes. *In* Biological Membranes. D. S. Parsons, editor. Clarendon Press, Oxford. 8–32.

Seaman, G. V. F., R. J. Knox, F. J. Nordt, and D. H. Regan. 1977. Red cell aging. I. Surface charge density and sialic acid content of density-fractionated human erythrocytes. *Blood.* 50:1001–1011.

Steck, T. L. 1974. The organization of proteins in the human red blood cell membrane. *J. Cell Biol.* 62:1–19.

Sweeley, C. C., and G. Dawson. 1969. Lipids of the erythrocyte. *In* Red Cell Membrane. G. A. Jamieson and T. J. Greenwalt, editors. J. B. Lippincott Company, Philadelphia. 172–227.

Tanner, M. J. A. 1978. Erythrocyte glycoproteins. *Curr. Top. Membr. Transp.* 11:279–325.

Tomita, M., and V. T. Marchesi. 1975. Amino acid sequence and oligosaccharide attachment sites of human erythrocyte glycophorin. *Proc. Natl. Acad. Sci. USA.* 72:2964–2968.

Uzgiris, E. E., and H. P. M. Fromageot. 1976. Thickness and density of protein films by optical mixing spectroscopy. *Biopolymers.* 15:257–263.

Vassar, P. S., J. M. Hards, and G. V. F. Seaman. 1973. Surface properties of human lymphocytes. *Biochim. Biophys. Acta.* 291:107–115.

Weinstein, R. S. 1974. The morphology of adult red cells. *In* The Red Blood Cell. D. M. Surgenor, editor. Academic Press, Inc., New York and London. 1:215–268.

Westerman, M. P., L. E. Pierce, and W. N. Jensen. 1961. A direct method for the quantitative measurement of red cell dimensions. *J. Lab. Clin. Med.* 57:819–824.

Whittam, R. 1964. Transport and Diffusion in Red Blood Cells. Arnold Publishers Ltd., London. 2.